Analysis of ADEOS-II GLI data by pattern decomposition method

Noriko Soyama*, Kanako Muramatsu†, Y.Xiong‡, Noboru Fujiwara‡

* Center for Research And Development of Liberal arts Education, Tenri University, Nara, Japan , Email:soyama@sta.tenri-u.ac.jp
† KYOU SEI Science Center and Department of Information and Computer Sciences, Nara Women's University, Nara, Japan
‡ Laboratory of Nature Information Science, Department of Information and Computer Sciences, Nara Women's University, Nara, Japan

Abstract

The Advanced Earth Observing Satellite-II (ADEOS-II) was successful launched on December 2002 by National Space Development Agency (NASDA) of Japan. Global Imager (GLI) aboard ADEOS-II is an optical sensor that observes reflected solar radiation and infrared radiation from Earth's surface with hyper-multi-channels. In this paper, we present results of the first analysis with GLI data using the pattern decomposition method (PDM), which is an analysis algorithm developed in multi-dimensional reflectance space and is suitable for sensor independent analysis. A set of spectral reflectance observed by GLI were successfully transformed into three pattern decomposition coefficients using PDM within 4% error per degree of freedom. Using these coefficients, vegetation index based on pattern decomposition (VIPD) was calculated, and seasonal change of vegetation was detected from VIPD image of February and June. From these result, ADEOS-II/GLI data is effective for monitoring the land cover types and vegetation changes.

Keywords: ADEOS-II/GLI, the pattern decomposition method, VIPD

1 Introduction

Human activities have rapidly changed land cover types and changed the natural cycles of energy and materials, causing environmental problems. It is important to understand the present situation and its influence.

Satellite sensor data is useful for monitoring the present situation of earth. The Advanced Earth Observing Satellite-II (ADEOS-II) was successful launched on December 2002 by National Space Development Agency (NASDA) of Japan. Global Imager (GLI) aboard ADEOS-II is an optical sensor that observes reflected solar radiation and infrared radiation from earth's surface with 36-spectral channels ranging from 0.38 to 12. micrometers. GLI has several channels, which wavelength are not included in the LANDSAT/TM spectral channels. Therefore, it is expected that GLI data give us valuable information about the land cover and also vegetation state.

We have developed an analysis algorithm, pattern decomposition method (PDM), for multi-dimensional data. With PDM, the multi-dimensional data of spectral reflectance is transformed into three dimensional data, such as water, vegetation and soil coefficients. As three coefficients almost directly correspond to ground objects, land cover types and quantitative changes in land cover can be held by classifying images based on the coefficients. Furthermore, Vegetation index based on pattern decomposition (VIPD) was also developed. It is useful for assessment of vegetation vigor, monitoring vegetation changes and estimation of net primary production of vegetation (NPP).

We have studied the applicability of the PDM to Landsat/TM and ETM+, and Terra/MODIS data and also spectral reflectance measured in the field. ADEOS-II/GLI data is just now available. In this paper, we study the effectiveness of GLI data for land area analysis and also applicability of PDM to hyper-multi-spectral GLI data.

2 Analysis algorithm

2.1 Pattern decomposition method

In the pattern decomposition method [1, 2, 3], a set of reflectance data of n-bands for each pixel was decomposed by a standard spectral patterns of water, vegetation and soil as follows,

$$A_i \rightarrow C_w P_{iw} + C_v P_{iv} + C_s P_{is}. \tag{1}$$

Hear A_i is a spectral reflectance of band i, P_{iw}, P_{iv} and P_{is} are the normalized standard spectral patterns for band i, that is normalized as $\sum_{i=1}^{n} |P_{ki}| = 1, (k = w, v, s)$, and n is number of band used for analysis. C_w, C_v and C_s are pattern decomposition coefficients of water, vegetation and soil, these are calculated using the least-square method with conditions, $C_w \geq 0, C_v \geq 0$ and $C_s \geq 0$.

Using the residual (R_i) of i band's reflectance,

$$R_i = A_i - \{C_w \cdot P_{iw} + C_v \cdot P_{iv} + C_s \cdot P_{is}\}, \tag{2}$$

the error index of the reduced-χ^2 for equation (1) is defined as follows,

$$\chi^2 = \sum_{i=1}^{n} R_i^2/(n-3), \tag{3}$$

where $(n-3)$ is the degree of freedom for a dataset of n-bands.

2.2 Vegetation Index based on Pattern Decomposition

VIPD [4, 5] is a vegetation index obtained by the pattern decomposition method, and is defined as follows,

$$VIPD = \frac{C_v - C_s - C_w \cdot \frac{S_s}{\sum_{i=1}^{n} A_i} + S_s}{S_v + S_s}. \tag{4}$$

Here, S_v and S_s are sum of reflectance data of standard vegetation and soil samples on all bands, respectively. By this definition, VIPD is zero for standard water or soil sample, while VIPD is one for standard vegetation sample. VIPD of a pixel is close to one, vegetation of selected area is more vigorous.

3 Data used in this study

3.1 GLI data and it's spectral channels used in this study

We used ADEOS-II/GLI data measured with 1km spatial resolution, shown as Figure 1 (a) and (b). It is false color image of the GLI data observed on Feb. 7 2003, and Jun. 3 2003, respectively. Band 28 (wavelength in short wavelength infrared range), 19 (wavelength in near infrared range) and 13 (wavelength in visible range), is displayed as red green and blue, respectively. Analyzed area in this study is around Kii peninsula (169×265 km) of Japan, and is inside the square in Figure 1.

(a) 2003/02/07 (b) 2003/06/03

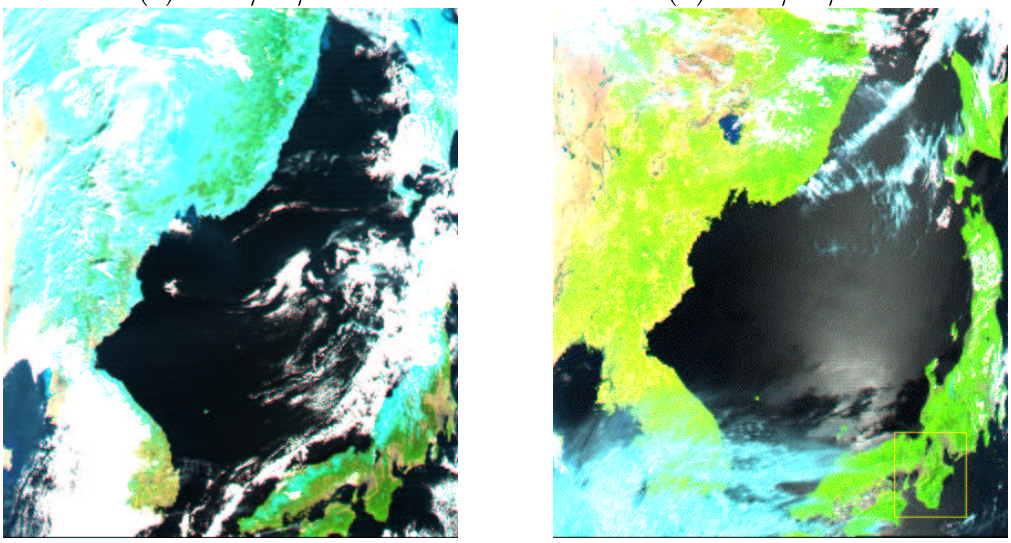

Figure 1: False color image of GLI(Pass:07, Scene:11)

In this study, we selected nine spectral channels, where light is not influenced strongly by water vapor and oxygen absorption, or aerosols in the atmosphere, from 19 spectral channels. The radiance of these 19 spectral channels is schedule to be provide as global mosaic data. Table 1 shows spectral bands used in this study with each channel number of ADEOS-II/GLI, wavelength, spectral width, and band number defined in this study.

Table 1: Characteristic of GLI spectral bands used in this study

Channel Number of GLI	Central Wavelength (nm)	Spectral Width (nm)	Band number defined in this study
1	380	10	1
5	460	10	2
8	545	10	3
13	678	10	4
15	710	10	5
19	865	10	6
24	1050	20	7
26	1240	20	8
28	1640	200	9

Spectral reduced reflectance A_i of band i was calculated from the radiance of GLI data as follows,

$$A_i = \frac{1}{L_i^{solar}}\{L_i - L_i^{path}\}, \tag{5}$$

where L_i $(Wm^{-2}sr^{-1}\mu m^{-1})$ is a spectral radiance observed by GLI, L_i^{path} $(Wm^{-2}sr^{-1}\mu m^{-1})$ is the spectral path radiance which is calculated using Rayleigh scattering[6], and L_i^{solar} $(Wm^{-2}\mu m^{-1}sr^{-1})$ is the spectral solar radiance at satellite altitude calculated as follows,

$$L_i^{solar} = \frac{E_i^{mean}\cos\theta_0}{\pi d^2}. \tag{6}$$

Here, E_i^{mean} $(Wm^{-2}sr^{-1}\mu m^{-1})$ is the solar spectral radiance of the band i at the mean earth-sun distance[7]. The value is published by ADEOS-II/GLI project. θ_0 is angle of sun from the zenith, d is earth-sun distance on the observation day in astronomical units.

Using the Equation (5), the spectral reflectance was calculated for GLI data measured on Feb. 7 and Jun. 3,2003. Figure 2 shows the spectral reflectance of nine channels for water (a), forest (b), and city area (c) samples on Feb. 7, and water (d), forest (e), and city area (f) on Jun. 3. Roughly speaking, we can see the typical spectral reflectance pattern of water, vegetation and soil from the Figure 2.

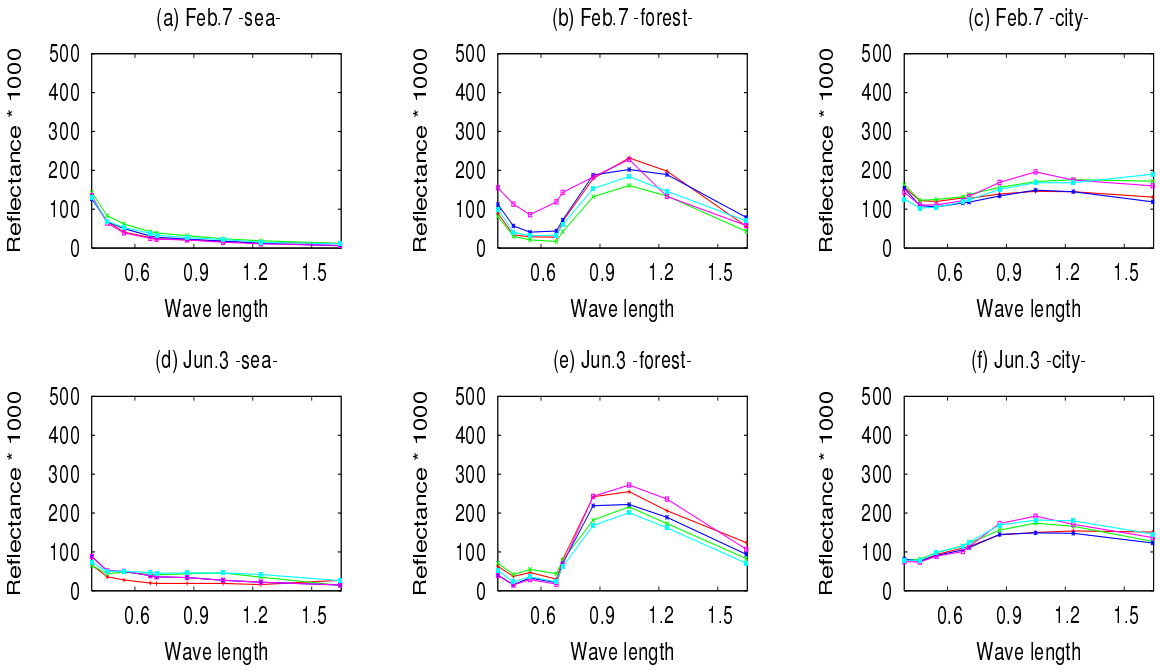

Figure 2: Spectral reflectance for nine GLI bands

3.2 Standard spectral patterns

Standard spectral patterns, P_{iw}, P_{iv}, and P_{is}, in Equation (1) are calculated from the standard samples of water, vegetation and soil measured in the field using a spectrometer. Figure 3 (a) shows extracted spectral reflectance of GLI nine channels for standard water, vegetation and soil samples. The samples are sea at Kata port, ten layers of green leaf of Quercus glauca and booming sand of Mingsha Mountain in Dunhuang. Figure 3 (b) shows the standard spectral patterns calculated from the reflectance data of Figure 3 (a).

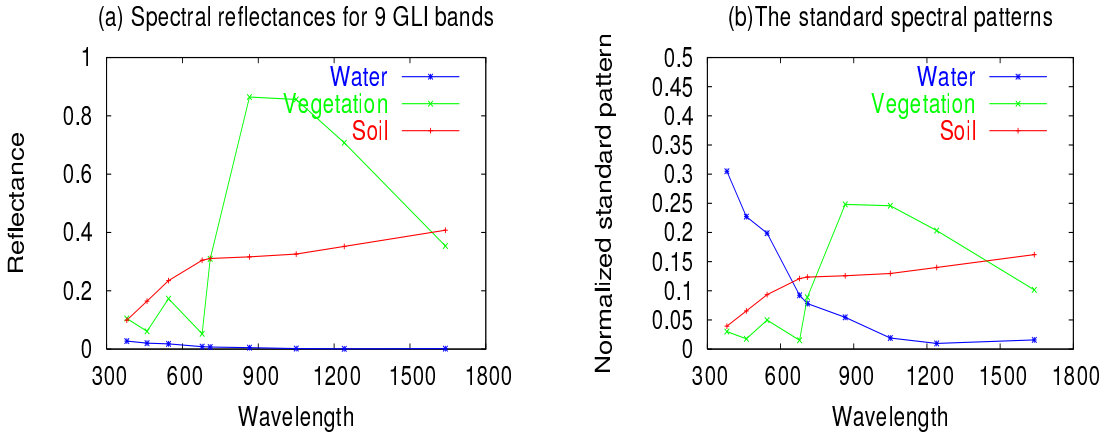

Figure 3: The spectral reflectance of nine GLI bands (a) and the standard spectral patterns used in this analysis (b).

4 Pattern decomposition analysis for GLI data

4.1 Results of pattern decomposition

Using the standard patterns shown in Figure 3 (b), GLI data measured on Feb. 7 and Jun. 3 was analyzed. Figure 4 shows the three pattern decomposition coefficients (C_w, C_v, C_s) and nine residuals $(R_i, i = 1, \ldots, 9)$ for the same samples shown in Figure 2. In Figure 4 (a) and (d), for the sea and lake samples, C_w is the largest among the three coefficients and the values are much smaller than those of the other samples. In Figure 4 (b) and (e), for the forest, C_v values is the largest among the three coefficients. In Figure 4 (c) and (f), and for the city, C_s is the largest. In comparison of C_v coefficients for two seasons', the values of C_v of Jun. are larger than Feb.'s. Thus, it seems that C_v reflects the maturity of vegetation. The residual for each sample is small.

Next, we studied the reduced-χ^2 for inside the square in Figure 1. Figure 5 shows the frequency distribution of χ^2 defined by equation(3) for every pixel of the analysis area. The average value of χ^2 is 0.001045 and 0.000264 for Feb. 7 and Jun. 3, respectively. The square root of 0.001045 is 0.032 (3.2%) and that of 0.000264 is 0.015 (1.5%). From these results, the reflectance of GLI nine channels can be fitted within the error of 4 %, in the pattern decomposition method. This result is almost same as the previous study using the spectral reflectance measured in the field.

In the pattern decomposition method, most of the information of GLI nine bands are transformed into three pattern decomposition coefficients. Using the coefficients, we made color composite image as shown in Figure 6. The coefficients for water, vegetation, soil are displayed as blue, green and red, respectively. Blue area correspond to sea, river and lake regions, green areas to forested regions and red areas to urban and bare soil regions.

Thus, the pattern decomposition method is sufficiently applicable to the analysis of the hyper-multidimensional GLI data and is expected to be useful for classification of land cover types.

4.2 Vegetation index based on pattern decomposition method

Figure 7 shows VIPD image of Kii peninsula using Equation (4). VIPD values are

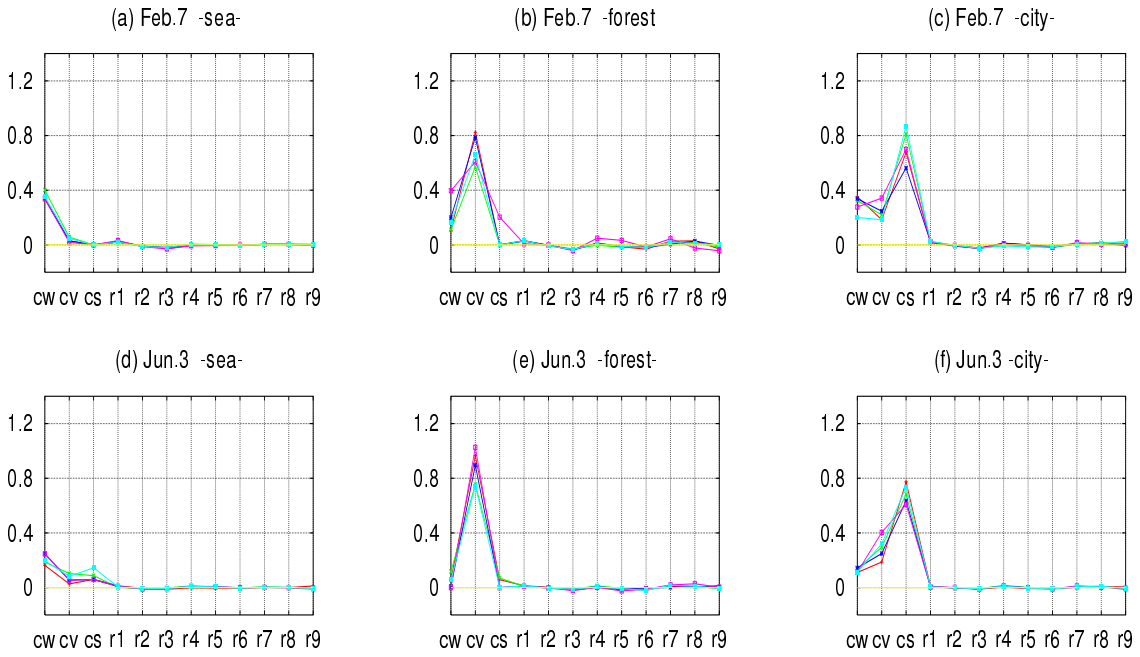

Figure 4: The pattern decomposition coefficients

displayed as gradation sequences shown in figure from black to white, in this case from -0.2 to 0.8.

In comparison of two VIPD maps of Figure 7(a) and (b), we can see that the value of VIPD of Jun. is higher than that of Feb. From this result, we can extract the seasonal change of vegetation state clearly using VIPD from GLI data. From this result, we can expect that VIPD is useful for detailed analysis of vegetation such as classification of vegetation type and estimation of net primary production of vegetation.

5 Conclusion

We show the first analysis result using GLI data and studied the applicability of pattern decomposition method to ADEOS-II/GLI data.

Nine spectral channels were selected 19 spectral channels. The radiance of the 19 spectral channels is scheduled to provide as global mosaic data with 1km spatial resolution. Roughly speaking, a set of spectral reflectance of nine channels were successfully transformed into three-dimensional data, namely water, vegetation, and soil pattern decomposition coefficients, within 4% error per degree of freedom. This result is almost same as the previous study using the spectral reflectance measured in the field. From this result, we can say that 96 % of information in the original reflectance data can be transformed into three coefficients using the method. Using the three coefficients, we show the color composite image of the coefficients for water, vegetation and soil displayed as blue, green and soil. From the results, we can say the three coefficients directly correspond to ground objects. We calculated VIPD using the data measured on Feb. 7 and Jun 3, and compared the results. The seasonal change of vegetation was clearly detected using VIPD.

From these result, ADEOS-II/GLI data is effective for monitoring the land cover

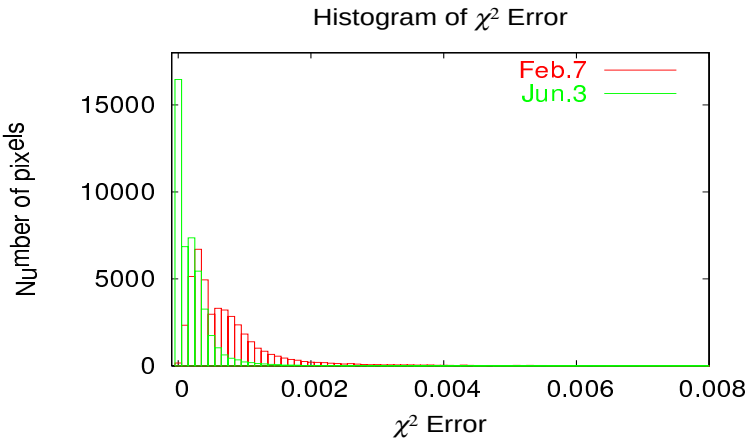

Figure 5: Frequency distribution of χ^2 for PDM with GLI data

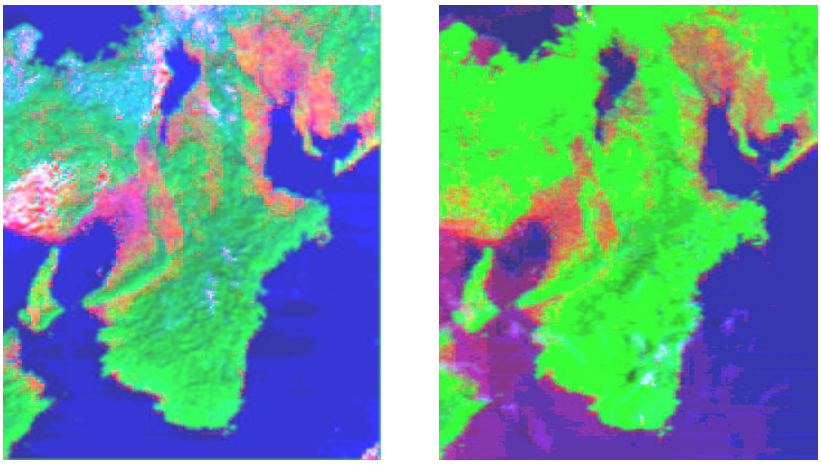

Figure 6: Color composite images of the coefficients for water, vegetation and soil displayed as blue, green and red respectively for (a) Feb.2 and (b) Jun.3

types and vegetation changes. We can expect that VIPD from GLI data is useful for detailed analysis of vegetation such as classification of vegetation type and estimation of net primary production of vegetation.

In the near future, we would like to classify land cover types and make a distribution map of NPP using GLI data. In the long term, we are going to construct a database which has information of land cover and vegetation changes and human activities.

We hope ADEOS-II/GLI data is satisfactory acquired.

Acknowledgements

This work was supported under the ADEOS-II/GLI project by the National Space Development Agency of Japan (NASDA) . We thank Dr.Hirokazu Yamamoto, NASDA, who always help us about GLI data.

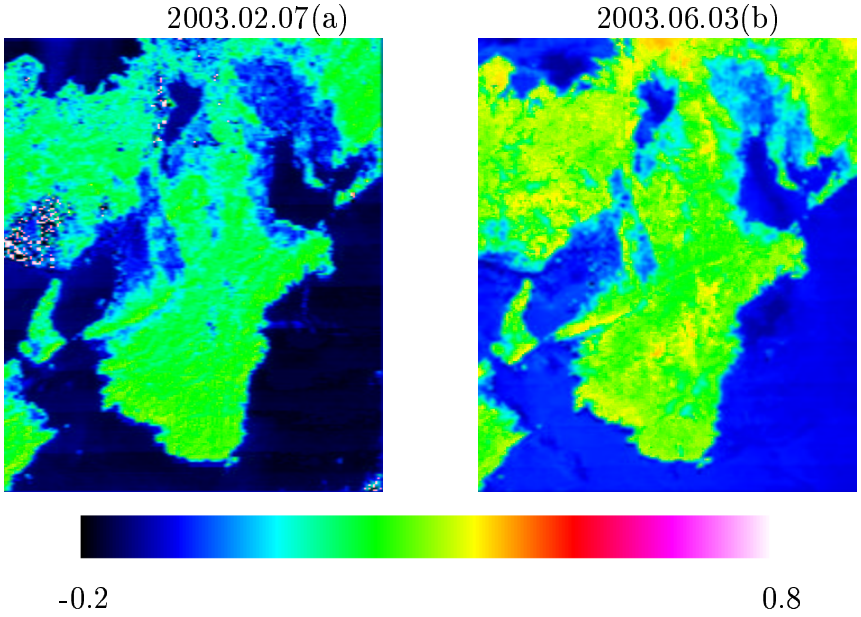

Figure 7: Distribution Map of Kii peninsula using VIPD

References

[1] Daigo, M., Ono, A., Fujiwara, N., Urabe, R. (2001). "Pattern expansion method for Hyper-multi-spectral data analysis" . in printed in *International Journal of Remote Sensing*.

[2] Fujiwara, N., Muramatsu, K., Awa, S., Hazumi,A. and Ochiai, F., (1996). "Pattern expansion method for satellite data analysis" (in Japanese). *Journal of Remote Sensing Society of Japan*, Vol.17, No.3, 17-37.

[3] Muramatsu,K., Furumi,S., Fujiwara,N., Hayashi, A., Daigo,M., Ochiai, F., (2000). "Pattern decomposition method in the albedo space for Landsat TM and MSS data analysis", *International Journal of Remote Sensing*, Vol.21, No.1, 99-119.

[4] Furumi, S., Hayashi, A., Muramatsu, K., Fujiwara, N., (1998). "Relatioin Between Vegetation Vigor and New Vegetation Index Based on Pattern Decomposition Method". *Journal of Remote Sensing Society of Japan*, Vol.18, No.3, 17-34.

[5] Hayashi A.,Muramatsu, K.,Furumi, S., Shiono Y., Fujiwara, N., Daigo M. , (1998). "An Algorithm and a New Vegetation Index for ADEOS-II/GLI Data Analysis". *Journal of Remote Sensing Society of Japan*, Vol.18, No.2, 28-50.

[6] Hill, J., Sturm, B., (1991). "Radiometric correction of multitemporal Thematic Mapper data for use in agricultural land-cover classification and vegetation monitoring". *International Journal of Remote Sensing*, Vol.7, 1471-1491.

[7] Markham, B.L., Barker, J.L., (1987). "Thematic Mapper bandpass solar exoatmospheric irradiances". *International Journal of Remote Sensing*, Vol.8, 517-523.